Adsorption of Hydrofluorocarbons HFC-134 and HFC-134A on X and Y Zeolites: Effect of Ion-Exchange on Selectivity and Heat of Adsorption

Scott Savitz, Flor R. Siperstein, Robert Huber, Stephen M. Tieri, Raymond J. Gorte, Alan L. Myers,* Clare P. Grey,† and David R. Corbin‡

Department of Chemical Engineering, University of Pennsylvania, Philadelphia, Pennsylvania 19104

Received: February 16, 1999; In Final Form: June 16, 1999

Adsorption isotherms and heats of adsorption were measured for HFC-134 (1,1,2,2-tetrafluoroethane) and HFC-134a (1,1,1,2-tetrafluoroethane) on a series of ion-exchanged (H, Li, Na, Rb, Cs) faujasites using volumetric and calorimetric techniques. The species and number of ions present in the zeolite strongly influence the heats of adsorption and the preferential adsorption of HFC-134 compared to HFC-134a. The selectivity is considerably higher in X than in Y zeolites because of the larger number of nonframework ions in X zeolites. The saturation capacity is six molecules per supercavity for both HFCs. The differences in observed heats of adsorption (except for RbX) can be explained by reasonable and consistent values of dispersion and ion−dipole electrostatic energies. The high selectivities for NaX and RbX indicate that either zeolite would be highly effective for gas separation.

1. Introduction

HFC-134a (CH_2FCF_3) is a hydrofluorocarbon coolant for refrigerators designated to replace the ozone-damaging chlorofluorocarbons (CFCs), whose use has been curtailed by the Montreal Protocol signed in 1987. The use of HFC-134a is growing rapidly as worldwide refrigerator and air-conditioner production rises almost exponentially.[1] A byproduct of HFC-134a production is the HFC-134 isomer (CHF_2CHF_2), which is unsuitable as a refrigerant fluid. The $C_2H_2F_4$ isomers are separated commercially by distillation, but their low relative volatility makes the process inefficient. Thus, investigating more efficient methods of separating the two isomers is important commercially. HFC-134 is adsorbed preferentially over HFC-134a on faujasites, making adsorption a potential alternative to distillation for this separation.[2] Measurements of isotherms and heats of adsorption of HFC-134 and HFC-134a on a range of zeolites are therefore useful for exploring possible adsorptive separation techniques. In addition, these data will provide insights regarding zeolite interactions with fluorinated species generally.

2. Experimental Section

Materials. Ion-exchanged X and Y zeolites were provided by DuPont Corporation. HY (with a bulk SiO_2/Al_2O_3 ratio of 85) was obtained from the PQ Corporation (vendor code CBV-780).

Exchange of both the X and Y zeolites was performed at 90 °C by contacting the zeolites with 8−10% nitrate solutions of the different cations (Li, K, Rb, and Cs) for 1 h. The exchange process was repeated between zero and three times.

Table 1 provides the zeolite composition per unit cell, as well as the number of moles of supercages per unit weight. (Note that there are eight supercages per unit cell.)

TABLE 1: Unit Cell Composition

zeolite	Si	Al	Na	M	mol sc/kg
LiX	110.5	81.5	13.98	60.1	0.65992
NaX	104.2	87.8	73.0	0.0	0.61543
RbX	105.6	86.4	38.8	42.6	0.50208
CsX	105.7	86.3	49.5	32.0	0.47638
HY	190.9	1.1	0.0	0.0	0.69347
LiY	135.7	56.3	15.6	29.5	0.66958
NaY	136.5	55.5	54.2	0.0	0.62940
CsY	133.2	58.8	24.6	30.5	0.49811

TABLE 2: Dehydration Factors

zeolite	dehydration factor	zeolite	dehydration factor
LiX	0.2580	HY	0.0594
NaX	0.2150	LiY	0.2230
RbX	0.1560	NaY	0.2380
CsX	0.1680	CsY	0.1750

The adsorbates, HFC-134 (1,1,2,2-tetrafluoroethane) and HFC-134a (1,1,1,2-tetrafluoroethane) were provided by DuPont. Impurities are less than 0.1 wt %.

Sample Pretreatment. The weights of the fully hydrated adsorbents were measured and their dehydrated masses were calculated using the dehydration factors given in Table 2. Dehydration factors, *f*, defined as

$$f = 1 - \frac{\text{dehydrated mass}}{\text{total mass}} \qquad (1)$$

were obtained by TGA (DuPont Instruments TGA model 951) up to 500 °C.

The sample size was about 0.8 g in the calorimeter and about 0.5 g in the volumetric apparatus. The experiments were performed on dehydrated zeolites. The bakeout procedure was to heat the sample from room temperature over a period of 24 h to 110 °C, then heat over a period of 12 h to 350−400 °C, and hold the sample at that temperature for another 12 h. Vacuum was maintained during the degassing.

Calorimeter. The combination of a calorimeter−volumetric apparatus described by Dunne et al. was used.[3] Samples of the

* Corresponding author.
† State University of New York at Stony Brook, Stony Brook, NY.
‡ DuPont Company, Central Research and Development, Experimental Station, Wilmington, DE 19880-0262.

10.1021/jp990560o CCC: $18.00
Published on Web 09/14/1999

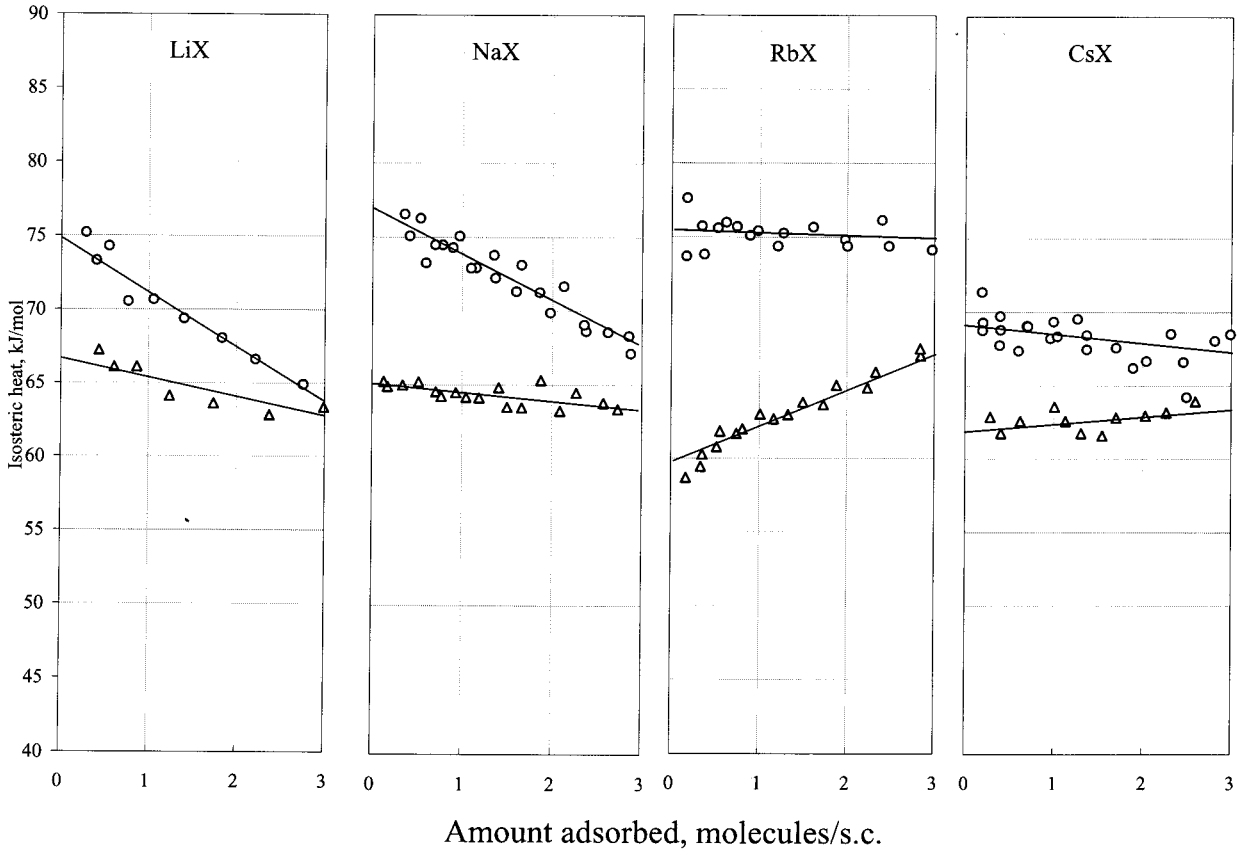

Figure 1. Isosteric heats of adsorption of HFC-134 (○) and HFC-134a (△) on X-type zeolites at approximately 25 °C.

zeolite powder were compressed into wafers. The dead space volume within the sample chamber was determined by helium expansions from the dosing loop. The adsorption isotherm and differential heat of adsorption were measured by introducing a known amount of HFC from the dosing loop into the sample cell. The differential heat of adsorption was obtained by numerically integrating the area under the response curve generated by the thermopiles. The adsorption isotherm was obtained by the volumetric procedure, based upon the difference between the amount introduced into the cell and the amount of gas remaining in the dead space of the cell at equilibrium. The quantity of gas adsorbed from a given dose of HFC was calculated by a mass balance,

$$\Delta n_{ads} = \frac{(P_d - P_{c,f})V_d}{RT_d} + \frac{(P_{c,i} - P_{c,f})V_c}{RT_c} \qquad (2)$$

where Δn_{ads} is the amount of gas adsorbed, P_d is the initial pressure in the dosing loop, $P_{c,i}$ and $P_{c,f}$ are, respectively, the initial and final pressures in the cell, T_c and T_d are the temperatures of the cell and dosing loop, and R is the gas constant. The loading is calculated by dividing Δn_{ads} by the mass of dehydrated adsorbent and adding this quantity to the loading measured for the previous point.

Reproducibility of the heats of adsorption within 3% was observed for additional experiments on the same sample and different samples. Attainment of equilibrium was checked by comparing points obtained by desorption and adsorption.

3. Results

Heats of Adsorption in X Zeolites. Isosteric heats of adsorption of HFC-134 and HFC-134a in zeolites LiX, NaX, RbX, and CsX are shown on Figure 1. Although the presence of Na cations in the Li-, Rb-, and Cs-exchanged forms of zeolite X makes the heats more difficult to interpret (see Table 1), the following general statements can be made.

(1) The heats of adsorption of HFC-134 are higher than the heats of adsorption of HFC-134a. The differences in heats at the limit of zero loading are 8, 12, 16, and 7 kJ/mol for LiX, NaX, RbX, and CsX, respectively. Thus, the difference in heats of adsorption as a function of the size of the cation passes through a maximum for RbX.

(2) The heat profile of HFC-134 is always more heterogeneous than the profile of HFC-134a. A positive slope is attributed to gas−gas (cooperative) interactions in combination with a relatively constant gas−solid interaction energy; a negative slope indicates heterogeneity in gas−solid interaction energies with a spectrum so wide that the cooperative interactions are concealed. A horizontal line indicates a balance between cooperative interactions and gas−solid energetic heterogeneity. The slope of the heat profile for HFC-134 is always less (algebraically) than for HFC-134a, indicating that the energies of adsorption sites extend over a wider spectrum for HFC-134 compared to HFC-134a. The highest degree of energetic heterogeneity is observed for HFC-134 on LiX and NaX. The most energetically uniform case of gas−solid interaction energy is for HFC-134a on RbX.

(3) The difference in heats decreases with loading.

The differences in isosteric heats of Figure 1 provide a basis for estimating the selectivity. The selectivity of the adsorbent for component 1 relative to component 2 is

$$s_{1,2} = \frac{x_1/y_1}{x_2/y_2} \qquad (3)$$

For a mixture of molecules of equal size, the selectivity of an

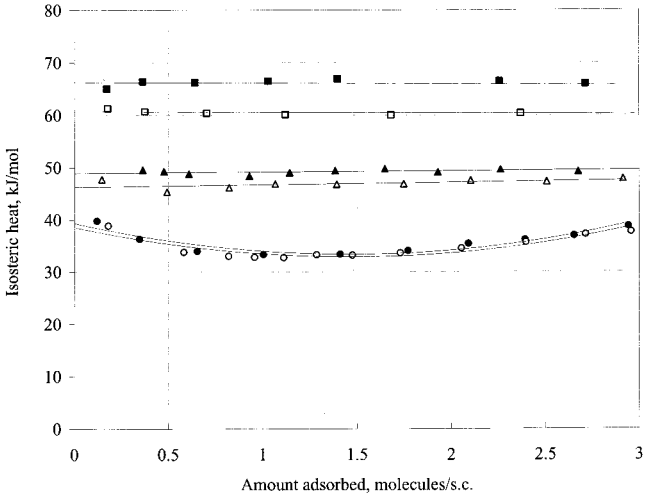

Figure 2. Isosteric heats of adsorption of HFC-134 (black symbols) and HFC-134a (open symbols) on Y-type zeolites: CsY (squares), LiY (triangles), HY (circles) at approximately 23 °C.

TABLE 3: Estimate of Selectivity of X Zeolites for Preferential Adsorption of HFC-134 Relative to HFC-134A at Limit of Zero Coverage and 25 °C

zeolite	Δq, kJ/mol	$s_{1,2}$
LiX	8	5
NaX	12	12
RbX	16	29
CsX	7	4

TABLE 4: Estimate of Selectivity of Y Zeolites for Preferential Adsorption of HFC-134 Relative to HFC-134A at Limit of Zero Coverage and 25 °C

zeolite	Δq, kJ/mol	$s_{1,2}$
HY	0	1.0
LiY	2.3	1.6
CsY	5.7	3.3

ideal solution is given by the difference in integral surface free energies,

$$\ln s_{1,2} = \frac{-(g_1 - g_2)}{RT} \tag{4}$$

Since differences in free energy are driven by differences in the energy of adsorption, selectivity may be correlated by

$$\ln s_{1,2} = \frac{-C(h_1 - h_2)}{RT} = \frac{C(q_1 - q_2)}{RT} \tag{5}$$

The value $C = 0.52$ predicts selectivities for a wide variety of binary mixtures on zeolites[4] within a factor of 2. Table 3 shows zero-coverage values of selectivity for the X series of zeolites. Since selectivity usually decreases with coverage, the values in Table 3 are maximum values. The high selectivities for NaX and RbX indicate that either zeolite would be highly effective for gas separation.

Heats of Adsorption in Y Zeolites. Isosteric heats of adsorption of HFC-134 and HFC-134a on HY, LiY, and CsY are plotted in Figure 2. The heats on HY are nearly indistinguishable. For LiY and CsY, both curves are flat but the heat for HFC-134 is higher than that for HFC-134a; the difference in the average heats over the range from zero to three molecules per supercage is given in Table 4. Selectivities predicted by eq 5 are also given in Table 4. Comparison of Tables 3 and 4 shows that the selectivity is considerably higher in X than in Y zeolites,

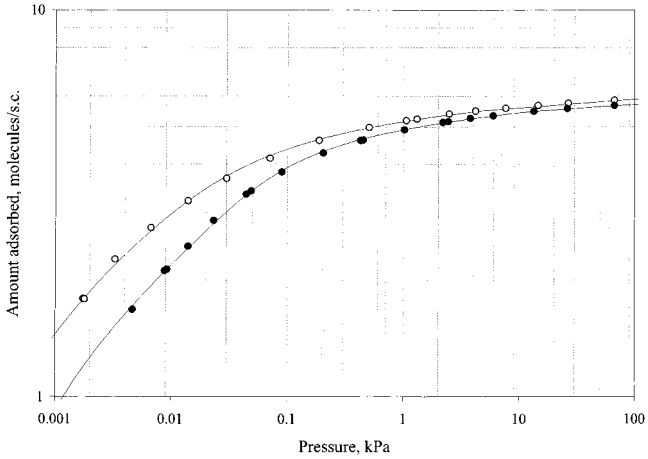

Figure 3. Isotherms on LiX at 50 °C: HFC-134 (○); HFC-134a (●).

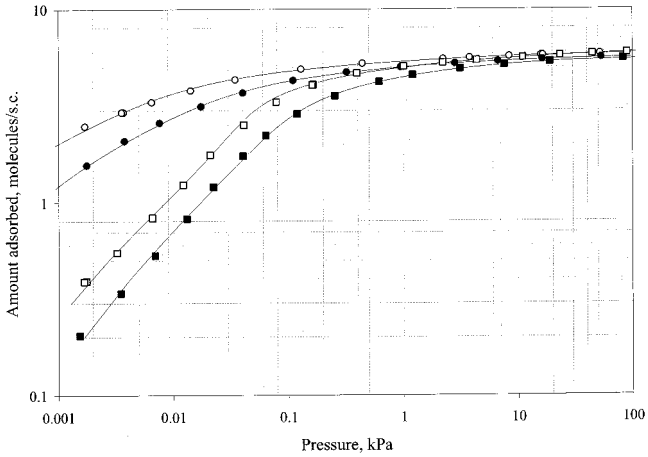

Figure 4. Isotherms on Na-exchanged FAU-type zeolites at 50 °C. NaX: HFC-134 (○), HFC-134a (●). NaY: HFC-134 (□), HFC-134a (■).

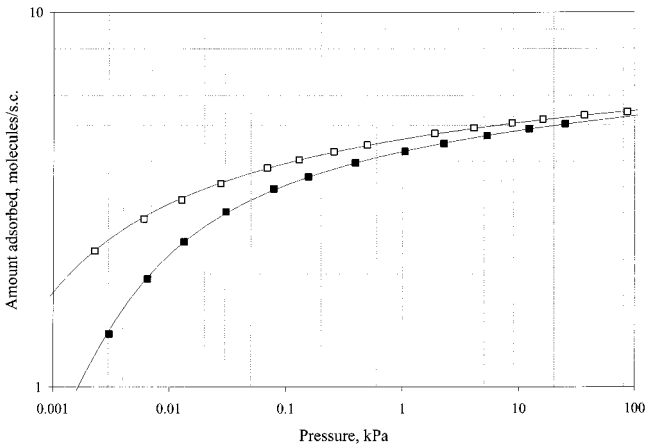

Figure 5. Isotherms on CsY at 50 °C: HFC-134 (□); HFC-134a (■).

as expected for the larger number of nonframework ions in X zeolites. However, the near constancy of the difference in heats of adsorption for Y zeolites means that their selectivity is nearly independent of loading.

Volumetric Results. Isotherms of HFC-134 and HFC-134a adsorbed in LiX, NaX, CsX, NaY, and CsY are shown in Figures 3−6. In all cases, HFC-134 is adsorbed preferentially over HFC-134a. However, the data at low coverage are insufficient for the determination of accurate values of Henry constants and consequently the selectivity cannot be calculated

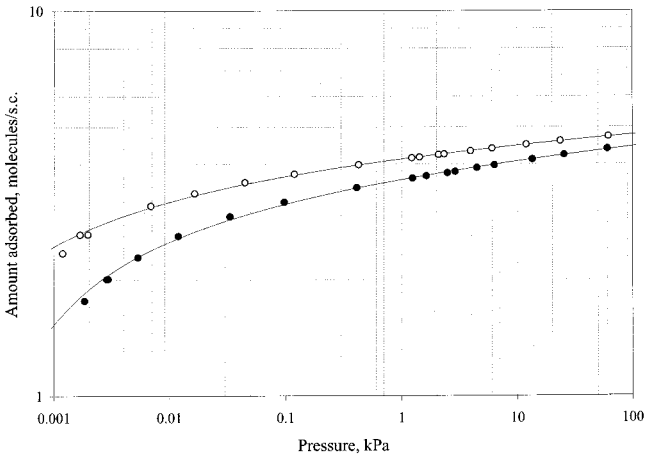

Figure 6. Isotherms on CsX at 50 °C: HFC-134 (○); HFC-134a (●).

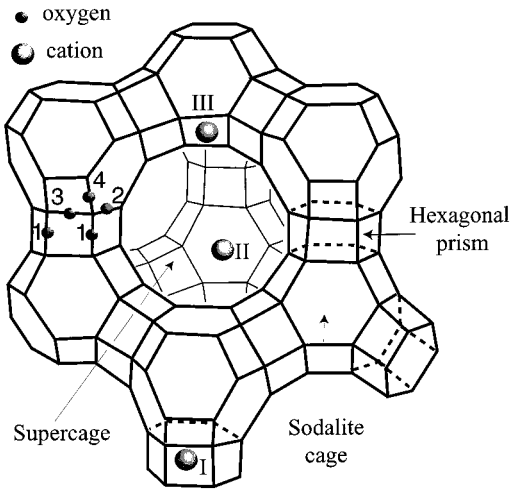

Figure 7. Faujasite structure showing cation sites (I, II, III) and locations of oxygen atoms (1, 2, 3, 4).

from the adsorption isotherms using ideal adsorbed solution (IAS) theory. The saturation capacity for both HFCs is six molecules per supercavity.

4. Discussion

The large variations in heats of adsorption for the different zeolites suggest a number of competing interactions. The major interaction besides dispersion is the electrostatic energy of the nonframework cations and the polar HFCs. HFC-134a has a dipole moment between 1.8 and 2.06 D.[5−6] The trans isomer of HFC-134 has no dipole moment, but the staggered-gauche isomer has a dipole moment estimated between 2.45 and 2.79 D.[5−8] Although the trans isomer is favored in the gas phase, earlier studies of HFC-134 sorbed on NaX[9,10] have demonstrated that the two isomers are present in a ratio of 2 to 1 (gauche/trans) at loading levels of four molecules per supercavity. The gauche/trans ratio increases to 3.3:1 at a loading level of two molecules per supercavity. From this, an even larger gauche/trans ratio may be expected at the limit of zero coverage. Thus, the selective adsorption of HFC-134 over HFC-134a is due to the higher dipole moment of the gauche isomer of HFC-134.

Figure 7 shows locations of oxygen atoms and nonframework cations in faujasite. Only sites I, II, and III are shown in the figure. Cations can also be found in sites I′, II′, and III′, which are slightly displaced from the ideal positions. Published information about the occupancies of cation sites for similar samples was used to infer the occupancy levels in Table 5 for the zeolites studied in this work. The distribution of the sodium ions in the partially exchanged X and Y zeolites is unknown.

TABLE 5: Cation Occupancy Data (per Supercage) for Sites in the Supercages of the Faujasite Structure with Similar Samples

	ions/supercage		occupancies			
sample	Na	M	SI/I′	SII/II′	SIII/III′	based on ref
HY			N/A	N/A	N/A	
LiY	1.95	3.69	3.69 Li			11, 12
NaY	6.78		2.78 Na	4.00 Na		13
CsY	3.08	3.81	0.06 Cs	3.06 Cs	0.69 Cs	14
LiX	1.75	7.51	3.51 Li	4.00 Li		11, 12
NaX	9.13		3.63 Na	3.63 Na	1.87 Na	15, 16
RbX	4.85	5.33	0.10 Rb	1.00 Rb	3.75 Rb	17
CsX	6.19	4.00		0.50 Cs	3.50 Cs	18

One of the main differences between dehydrated NaX and NaY is the abundance of Na ions in positions close to SIII in NaX not found in NaY.[13,19] It is important to note that the distribution of cations in Y zeolites depends on the size (and nature) of the ions. For example, for partially exchanged LiY zeolites, all Li ions are found mainly in SI/I′;[11,12] for NaY there is a larger occupancy of Na ions in SII than in SI/I′,[13] and for CsY, Cs cations are mainly found in SII and some in SIII.[14] The difference in ion locations between Li- and Cs-exchanged Y zeolites can explain the difference in heats of adsorption of the HFCs. Lithium ions in site II buried between the oxygens of the six-membered ring are inaccessible to the adsorbates,[20,21] whereas larger ions in SII are accessible to adsorbate molecules in the supercage.[22] Therefore, the heats of adsorption and the difference between the heats of adsorption of both HFCs are smaller in LiY than in CsY.

The distribution of ions is also important in ion-exchanged X zeolites. Li ions are not found in SIII for exchanges containing less than about 70% of Li in for LiNaLSX.[20,21] In contrast, in partially Cs-exchanged X zeolites, there is a high occupancy of Cs ions in SIII while Na ions occupy mainly SI/I′ and SII.[18] Despite the similar occupancies of Rb and Cs cations in X zeolites, the behavior of HFCs is quite different; evidently size and stearic factors are important for these systems. The nearly equal heats of adsorption on CsX and CsY zeolites may be due to the presence of approximately the same number of Cs ions in the easily accessible SII and SIII positions.[18,22]

Molecular simulations are needed to provide a satisfactory explanation of the behavior of these systems. The molecular model is complicated by incomplete information about the locations of the cations in these X and Y zeolites. It is worthwhile to consider whether the observed heats and selectivities can be explained by differences in electrostatic energies between the nonframework cations and the polar HFC molecules.

The magnitude of the electrostatic energies in Y zeolites was estimated from Figure 2. The negative charges on the oxygen atoms of the zeolite partially offset the positive charge of the exchangeable cations so that their effective charge is less than unity. HY zeolite is nearly free of nonframework ions (see Table 1), and London dispersion energy is the main contribution to the heat of adsorption. Assuming that the electrostatic energy for adsorption of HFC-134 and HFC-134a is negligibly small, the dispersion energy is about 35 kJ/mol in all zeolites. The leading term for electrostatic energy in these systems is the ion−dipole interaction,

$$U = \frac{q\mu \cos\theta}{r^2} \tag{6}$$

TABLE 6: Cationic Charge in X-Type Zeolites Calculated from Eq 6 (Values Are Fraction of Unit Positive Charge)

molecule	LiX	NaX	RbX	CsX
HFC-134	0.65	0.66	0.66	0.55
HFC-134a	0.68	0.66	0.54	0.59

where q is the effective charge of the cation, μ is the dipole moment of the HFC molecule, and r is the ion−dipole distance. Assume that the dipole moment is favorably oriented to the cation so that $\theta = 0$, $r = 3.5$ Å, and the dipole moment of the HFC-134a is the average of the values quoted above, $\mu = 1.93$ D. The electrostatic contribution to the heat of adsorption was obtained by subtracting the average dispersion energy in HY (35 kJ/mol) from the average isosteric heat of adsorption of HFC-134a in LiY and CsY (46.9 and 60.5 kJ/mol, respectively). The effective charge of the cations from eq 6 is 0.26*e* in LiY and 0.56*e* in CsY. Thus, the large increase in energy in Y-type zeolites going from HY to CsY can be explained by ion−dipole electrostatic interaction. The difference in heats between HFC-134a and HFC-134 in LiY implies that 89% of the adsorbed HFC-134 molecules are in the gauche configuration at the limit of zero coverage, which is consistent with previous work.[9,10]

Since the locations of the oxygen atoms are practically the same in X and Y zeolites, the dispersion energy should be approximately 35 kJ/mol in both zeolites. Assuming that HFC-134 molecules are all gauche isomers at the limit of zero coverage, the dipole moments of HFC-134 and HFC-134a are approximately the average of the values quoted above, 2.62 and 1.93 D, respectively. Assuming as before that $\theta = 0$ and $r = 3.5$ Å, eq 6 yields effective charges given in Table 6 for the HFCs. If the HFC molecules were identical, they would select the same site and orientation at zero coverage and the calculated charges would be identical. The values obtained in LiX, NaX, and CsX are the same for both HFCs within 7%. However, the 20% lower value of effective charge calculated for HFC-134a in RbX is unexplained.

5. Conclusion

HFC-134 is adsorbed preferentially relative to HFC-134a in all X and Y zeolites studied except for HY. The higher dipole moment of HFC-134 (in its gauche form) compared to HFC-134a is the main reason for the preferential adsorption of HFC-134. The differences in observed heats of adsorption (except for RbX) can be explained by reasonable and consistent values of dispersion and ion−dipole electrostatic energies. In general, the selectivity is higher in X zeolites than in Y zeolites because of the presence of cations in SIII. RbX has the highest selectivity for the systems studied.

Acknowledgment. This work was supported by National Science Foundation Grant CTS 96-10030. Technical assistance of Penrose Hollins is acknowledged.

Appendix

Heats of Adsorption

n (molec/s.c.)	*Q*st (kJ/mol)	*n* (molec/s.c.)	*Q*st (kJ/mol)	*n* (molec/s.c.)	*Q*st (kJ/mol)
HFC-134 on LiX (0.6575 g) at 25.2 °C					
0.154	78.3	0.768	70.5	2.216	66.6
0.285	75.2	1.059	70.6	2.756	64.9
0.407	73.3	1.407	69.4		
0.548	74.3	1.836	68.0		
HFC-134a on LiX (0.6575 g) at 27.4 °C					
0.154	68.8	0.608	66.1	1.741	63.6
0.304	70.0	0.866	66.1	2.376	62.8
0.436	67.2	1.241	64.1	2.989	63.4
HFC-134 on NaX (0.6832 g) at 26.2 °C					
0.416	75.1	1.368	72.2	2.621	68.6
0.595	73.2	1.604	71.3	2.877	67.1
0.782	74.5	1.858	71.3	3.159	67.0
0.967	75.1	2.131	71.7		
1.154	72.9	2.379	68.6		
HFC-134 on NaX (0.6832 g) at 30.3 °C					
0.356	76.5	1.098	72.9	2.360	69.1
0.531	76.3	1.354	73.8	2.854	68.3
0.702	74.5	1.661	73.1	3.377	66.5
0.898	74.3	1.981	69.9		
HFC-134a on NaX (0.6832 g) at 25.7 °C					
0.171	64.9	0.708	64.5	1.876	65.3
0.340	64.9	1.193	64.1	2.271	64.5
0.517	65.2	1.501	63.5		
HFC-134a on NaX (0.6832 g) at 28.9 °C					
0.129	65.2	1.408	64.8	2.572	63.8
0.771	64.2	1.662	63.5	3.090	62.2
1.047	64.1	2.086	63.2		
HFC-134 on RbX (0.5908 g) at 22.1 °C					
0.173	77.6	0.981	75.4	2.401	76.1
0.342	75.8	1.274	75.3	3.322	76.3
0.525	75.6	1.610	75.7		
0.742	75.7	1.978	74.8		
HFC-134 on RbX (0.5908 g) at 22.2 °C					
0.168	73.7	0.890	75.1	2.481	74.4
0.373	73.8	1.208	74.4	2.972	74.1
0.618	76.0	2.005	74.4	3.470	72.4
HFC-134a on RbX (0.5908 g) at 22.1 °C					
0.170	58.7	1.165	62.7	2.846	67.0
0.353	60.2	1.502	63.8	3.442	68.4
0.558	61.8	1.882	65.0		
0.811	62.0	2.333	65.8		
HFC-134a on RbX (0.5908 g) at 22.8 °C					
0.341	59.4	1.015	63.0	2.237	64.8
0.519	60.7	1.332	63.0	2.839	67.4
0.741	61.7	1.735	63.6		
HFC-134 on CsX (0.7362 g) at 22.1 °C					
0.195	69.3	0.958	68.2	2.459	66.6
0.388	69.7	1.366	67.4	3.036	65.6
0.599	67.4	1.895	66.2		
HFC-134 on CsX (0.7362 g) at 22.3 °C					
0.194	68.7	0.993	69.3	2.811	68.0
0.393	68.8	1.264	69.5	3.416	67.4
0.691	69.0	2.320	68.5		
HFC-134 on CsX (0.7362 g) at 22.0 °C					
0.189	71.3	1.036	68.3	2.043	66.6
0.383	67.7	1.365	68.4	2.494	64.2
0.705	69.0	1.699	67.6	2.989	68.5
HFC-134a on CsX (0.7362 g) at 21.2 °C					
0.400	61.8	1.542	61.6	2.597	63.9
1.127	62.6	2.032	63.0	3.202	64.5
HFC-134a on CsX (0.7241 g) at 24.6 °C					
0.281	62.8	1.002	63.6	1.701	62.8
0.620	62.6	1.306	61.7	2.266	63.2
HFC-134 on High-Silica Zeolite Y (0.8281 g) at 22.2 °C					
0.119	39.8	1.410	33.4	2.654	36.9
0.347	36.3	1.769	34.0	2.943	38.7
0.653	34.0	2.090	35.4	3.255	39.9
1.004	33.4	2.394	36.2		

Heats of Adsorption

n (molec/s.c.)	*Q*st (kJ/mol)	*n* (molec/s.c.)	*Q*st (kJ/mol)	*n* (molec/s.c.)	*Q*st (kJ/mol)
HFC-134 on High-Silica Zeolite Y (0.8281 g) at 24.5 °C					
0.179	38.9	1.111	32.7	2.053	34.5
0.582	33.8	1.285	33.3	2.397	35.7
0.820	33.0	1.475	33.2	2.716	37.2
0.957	32.8	1.728	33.6	2.958	37.7
HFC-134 on LiY (0.7284 g) at 22.6 °C					
0.363	49.6	1.142	49.0	2.263	49.6
0.476	49.2	1.384	49.4	2.677	49.2
0.609	48.8	1.647	49.7		
0.930	48.4	1.928	49.1		
HFC-134a on LiY (0.7284 g) at 21.2 °C					
0.145	47.8	1.391	46.8	2.915	47.9
0.493	45.3	1.747	46.8	3.327	48.1
0.823	46.1	2.104	47.5		
1.066	46.8	2.509	47.3		
HFC-134 on CsY (0.7318 g) at 24.7 °C					
0.172	65.1	1.028	66.5	2.713	66.0
0.363	66.4	1.396	66.9	3.122	64.6
0.639	66.3	2.258	66.5		
HFC-134a on CsY (0.7318 g) at 25.9 °C					
0.176	61.3	1.119	60.1	3.033	60.7
0.374	60.7	1.680	60.1		
0.703	60.4	2.370	60.3		

Adsorption Isotherms

P (Pa)	*n* (mol/kg)	*P* (Pa)	*n* (mol/kg)	*P* (Pa)	*n* (mol/kg)
HFC-134 on LiX (0.3707 g) at 50.4 °C					
1.75	1.790	70.9	4.143	4208	5.494
1.8	1.788	187.3	4.611	7658	5.588
3.29	2.266	503.9	4.981	14590	5.676
6.71	2.737	1307	5.241	26607	5.753
14.09	3.214	1055	5.196	66800	5.852
30.03	3.675	2484	5.402		
HFC-134a on LiX (0.3707 g) at 50.4 °C					
4.66	1.680	89.47	3.816	2433	5.163
9.2	2.131	202.7	4.279	5965	5.346
8.81	2.118	450.1	4.626	13388	5.481
13.99	2.449	426.1	4.610	26043	5.576
23.31	2.861	1021	4.913	66794	5.683
49.09	3.413	2191	5.140		
44.53	3.347	3780	5.260		
HFC-134 on NaX (0.3695 g) at 51.7 °C					
1.7	2.490	34.65	4.324	8386	5.683
3.69	2.935	129.1	4.890	15980	5.749
3.56	2.932	439.5	5.227	52130	5.847
6.48	3.312	2216	5.510	16510	5.747
14.20	3.804	3796	5.590		
HFC-134 on NaX (0.3695 g) at 72.1 °C					
0.75	1.275	20.19	3.093	2048	5.233
2.18	1.822	42.71	3.583	10260	5.503
1.97	1.821	97.34	4.094	24670	5.616
4.46	2.223	264	4.608	61510	5.694
10.36	2.683	627	4.928		
HFC-134 on NaX (0.3695 g) at 92.5 °C					
1.48	1.021	90.68	3.307	1461	4.861
3.49	1.404	129.4	3.544	3612	5.142
3.34	1.401	192.0	3.806	6565	5.288
7.70	1.877	305.0	4.101	15700	5.451
17.04	2.284	490.0	4.369	63050	5.630
42.25	2.854	839.0	4.636		
HFC-134a on NaX (0.3695 g) at 51.9 °C					
0.99	1.162	17.46	3.144	2821	5.229
0.86	1.162	40.32	3.700	6717	5.359
1.77	1.566	110.1	4.277	16330	5.471
3.76	2.085	321.3	4.721	53440	5.600
7.61	2.587	946.7	5.020		

Adsorption Isotherms

P (Pa)	*n* (mol/kg)	*P* (Pa)	*n* (mol/kg)	*P* (Pa)	*n* (mol/kg)
HFC-134a on NaX (0.3695 g) at 72.2 °C					
1.72	0.864	45.59	2.852	4190	5.023
1.54	0.863	90.09	3.320	10970	5.204
3.13	1.190	184.0	3.766	18010	5.280
6.11	1.550	384.0	4.188	43480	5.388
11.61	1.968	889.5	4.573	74890	5.436
23.12	2.402	1814	4.814		
HFC-134a on NaX (0.3695 g) at 92.4 °C					
1.33	0.367	82.29	2.432	7475	4.878
1.26	0.365	136.2	2.771	14120	5.029
2.01	0.533	275.3	3.255	39460	5.210
5.24	0.881	495.0	3.647	74720	5.289
10.28	1.219	744.9	3.902		
20.96	1.590	1665	4.333		
41.34	1.987	1671	4.331		
HFC-134 on CsX (0.4876 g) at 50.4 °C					
1.18	2.346	118.9	3.768	3927	4.328
1.96	2.625	425.1	3.987	6043	4.393
1.67	2.623	1226	4.154	11970	4.495
6.85	3.113	2083	4.237	23490	4.591
16.39	3.355	1424	4.172	61396	4.720
44.49	3.581	2323	4.248	101180	4.779
HFC-134a on CsX (0.4876 g) at 50.4 °C					
1.84	1.763	96.91	3.185	4457	3.915
2.93	2.010	409.7	3.475	6315	3.973
2.87	2.006	1242	3.673	13500	4.113
5.31	2.288	2480	3.798	25350	4.230
11.85	2.601	1635	3.726	60190	4.376
33.13	2.923	2889	3.825	100540	4.457
HFC-134 on NaY (0.3691 g) at 51.3 °C					
1.76	0.391	41.11	2.519	2219	5.278
1.68	0.389	78.63	3.310	4379	5.434
3.27	0.547	164.4	4.060	11060	5.610
6.59	0.833	161.3	4.052	23440	5.736
12.21	1.232	396.4	4.658	44690	5.829
20.98	1.758	1003	5.048	89720	5.931
HFC-134 on NaY (0.3691 g) at 91.0 °C					
0.92	0.074	51.62	0.659	1140	3.657
0.86	0.073	89.92	0.954	3311	4.448
1.72	0.107	146.2	1.325	6279	4.768
4.38	0.176	237.3	1.824	12070	5.016
10.4	0.274	401.1	2.447	23120	5.209
HFC-134a on NaY (0.3691 g) at 50.4 °C					
1.54	0.204	40.46	1.742	1202	4.564
3.52	0.338	63.65	2.218	3127	4.921
6.97	0.529	118.7	2.875	7607	5.146
13.16	0.824	254.5	3.567	19090	5.325
22.48	1.203	613.6	4.204	83030	5.529
HFC-134a on NaY (0.3691 g) at 92.0 °C					
4.6	0.069	100.4	0.626	2951	3.548
4.28	0.066	164.0	0.888	6969	4.134
7.38	0.099	257.3	1.213	21830	4.693
13.81	0.154	488.6	1.822	51930	4.971
30.09	0.269	878.8	2.432	111500	5.127
50.42	0.381	1571	3.013		
HFC-134 on CsY (0.4681 g) at 52.1 °C					
0.87	1.767	69.34	3.840	4114	4.918
2.28	2.305	130.0	4.042	8756	5.066
6.05	2.806	257.1	4.245	16170	5.178
12.79	3.159	497.7	4.424	37000	5.312
27.63	3.492	1896	4.750	87560	5.421
HFC-134 on CsY (0.4681 g) at 91.5 °C					
0.96	0.503	67.33	2.696	6724	4.362
0.87	0.502	132.0	3.024	13180	4.530
1.76	0.737	320.0	3.410	28260	4.699
3.17	1.063	613.6	3.656	56210	4.834
11.37	1.744	1252	3.899	96220	4.934
28.28	2.251	2822	4.129		

Adsorption Isotherms

P (Pa)	*n* (mol/kg)	*P* (Pa)	*n* (mol/kg)	*P* (Pa)	*n* (mol/kg)
HFC-134a on CsY (0.4681 g) at 51.7 °C					
0.53	0.434	13.43	2.439	2271	4.468
0.96	0.684	30.60	2.933	5349	4.687
0.85	0.683	78.63	3.375	12340	4.882
1.58	0.963	156.0	3.638	25300	5.040
3.03	1.385	393.6	3.965		
6.47	1.940	1049	4.256		
HFC-134a on CsY (0.4681 g) at 91.6 °C					
1.54	0.130	25.40	1.148	3238	3.764
1.47	0.128	50.10	1.603	8511	4.063
2.24	0.181	109.6	2.128	17880	4.272
3.58	0.280	311.4	2.778	34510	4.444
6.96	0.479	700.8	3.183	87790	4.652
12.86	0.752	1473	3.488		

References and Notes

(1) Hileman, B. A Chilling Battle. *Chem. Eng. News* **1998**, 33−34.

(2) Corbin, D. R.; Mahler, V. A. U.S. Patent 5,600,040, July 17, 1995.

(3) Dunne, J. A.; Mariwala. R.; Rao, M.; Sircar, S.; Gorte, R. J.; Myers, A. L. *Langmuir* **1996**, *12*, 5888−5895.

(4) Siperstein, F.; Myers, A. L. Experimental thermodynamic functions of mixing for enthalpy, free energy, and entropy of 7 binary gas mixtures adsorbed on zeolites, in preparation (1999).

(5) Papasavva, S.; Illinger, K. H.; Kenny J. E. *J. Phys. Chem.* **1996**, *100*, 10100−10110.

(6) Meyer, C. W.; Morrison, G. *J. Phys. Chem.* **1991**, *95*, 3860−3866.

(7) Brown, D. E.; Beagley, B. J. *Mol. Structure* **1977**, *39*, 167−176.

(8) Klaboe, P.; Nielsen, J. R. *J. Chem. Phys.* **1960**, *32*, 899−907.

(9) Crawford, M. K.; Dobbs, KD, Smalley, R. J.; Corbin, D. R.; Maliszewskyj, N.; Udovic, T. J.; Cavanagh, R. R.; Rush, J. J.; Grey, C. P. *J. Phys. Chem. B* **1999**, *103* (3), 431−434.

(10) Udovic, T. J.; Nicol, J. M.; Cavanagh, R. R.; Rush, J. J.; Crawford, M. K.; Grey, C. P.; Corbin, D. R. *Mater. Res. Soc. Symp. Proc.* **1995**, *376* (Neutron Scattering in Materials Science II), 751−756.

(11) Forano, C.; Slade, R. C. T.; Krogh Anderson, E.; Krogh Anderson, I. G.; Prince, E. J. *J. Solid State Chem.* **1989**, *82*, 95.

(12) Gillot, B.; El Guendouzi, M.; Laarj, M.; Tailhades, P.; Rousset, A. *J. Mater. Sci.* **1988**, *23*, 3342.

(13) Godber, J.; Baker, M. D.; Ozin, G. A. *J. Phys. Chem.* **1989**, *93*, 1409−1421.

(14) Norby, P.; Poshni, F. I.; Gualtieri, A. F.; Hanson, J. C.; Grey, C. P. *J. Phys. Chem B* **1998**, *102*, 839−856.

(15) Olson, D. H. *Zeolites* **1995**, *15*, 439−443.

(16) Takaishi, T. *Zeolites* **1996**, *17*, 389−392.

(17) Lee, S. H.; Kim, Y.; Kim, D. S.; Seff, K. *Bull. Korean Chem. Soc.* **1998**, *19* (1), 98.

(18) Shepelev, Y. F.; Butikova, I. K.; Smolin, Y. I. *Zeolites* **1991**, *11*, 287.

(19) Fitch, A. N.; Jobic, H.; Renoprez, A. *J. Phys. Chem.* **1986**, *90*, 1311.

(20) Gaffney, T. R. *Curr. Opin. Solid State Mater. Sci.* **1996**, *1*, 69−75.

(21) Geuerstein, M.; Engelhardt, G.; McDaniel, P. L.; MacDougall, J. E.; Gaffney, T. R. *Microporous Mesoporous Mater.* **1998**, *26*, 27−35.

(22) Ramamurthy, V.; Eaton, D. F. In *Proceedings of the 9th International Zeolite Conference*; Von Ballmoos, R., Higgins, J. B., Treacy, M. M. J., Eds.; Butterworth-Heinemann: Boston, MA, 1993; pp 587−594.